www.amlett.org, www.amlett.com, DOI: 10.5185/amlett.2012.icnano.259
"ICNANO 2011" Special Issue Published online by the VBRI press in 2012

Electron spin resonance in electrodeposited cobalt nanowire arrays

Sachin Pathak and Manish Sharma*

Centre for Applied Research in Electronics, Indian Institute of Technology, Delhi, New Delhi 110016, India

*Corresponding author. Tel: (+91) 11-26596036; E-mail: manish@care.iitd.ac.in

ABSTRACT

Arrays of magnetic nanowires electrodeposited into nano-channel templates have attracted a lot of attention and research efforts in recent years. They are a promising system for perpendicular magnetic recording media. A major issue regarding the fabrication of such nanowires is the interplay between the structure and magnetic properties. In this paper template-assisted electrodeposition technique using a three-electrode electrochemical cell is used to produce high density cobalt nanomaterial arrays with cylindrical shapes. The morphology of the samples is investigated by means of Scanning electron microscopy (SEM) and Transmission electron microscopy (TEM). The length and average diameter of Cobalt nanowire arrays was found 4–15 µm and ~300 nm, respectively. The structural characteristic of the samples is examined using XRD and EDX, which confirm the hexagonal closely packed cobalt array structures. Magnetic property measurements show the influence of morphology on the magnetic properties of the arrays. Magnetic characterizations were carried out by Magneto-optical Kerr Effect (MOKE) and Electron paramagnetic resonance (EPR). The experimental results suggest close agreement with the resonance field seen in micro-magnetic modelling. We have calculated the resonance field for single nanowires with different length and for an array of seven nanowires. It is shown that the resonance field varies with the length, the interaction strength and also the spacing of the nanowires.

Keywords: Electrodeposition; magnetic nanowire; electron spin resonance; magneto-optical kerr effect.

Sachin Pathak was born in Moradabad, Uttar Pradesh, India in 1983. He received his Graduation and Post graduation degrees in Physics with Electronics as a special subject from M. J. P. Rohilkhand University, Bareilly, India, in 2004 and 2006 respectively. He was awarded research fellowship by Council of Scientific and Industrial Research (CSIR), New Delhi in 2008. He is presently a research scholar at IIT Delhi Delhi, India. In Experimental Condensed Matter Physics, his present interests are in patterned magnetic media, and magneto-optic properties of magnetic nanostructures.

Manish Sharma received his B. Tech. (Hons.) from IIT Kharagpur in 1991 and his M.S. and Ph.D. from Stanford University, USA in 1996 and 2000, all in Electrical Engineering. During 2000-2006, he worked at Hewlett-Packard Research Labs, Palo Alto, USA, where his research interests were in magnetic materials for non-volatile Magnetic Random Access Memory and biological sensors. Since 2006, he has been with IIT Delhi, where he is currently an Associate Professor.

Introduction

The investigation of magnetization switching behaviour in magnetic metallic nanostructures like nanowires or nanotubes has attracted wide interest in both fundamental physics and nanotechnology. In recent years, the fabrication of arrays of pure metal nanowires, multilayered nanowires and alloy nanowires have gained enormous attention due to their superior properties, including magnetic sensor, perpendicular magnetic anisotropy and enhanced coercivity [**1-3**]. Magnetic nanowires are also increasingly draw interest in particular for biological and biomedical applications [**4, 5**]. In this paper, we have investigated the influence of the key magnetic properties (shape, magnetocrystalline anisotropy, magnetostriction, magnetostatic interactions) of the arrays of Co nanowire. These properties strongly affected by the different magnetic materials as well as on the shape of the nanostructures. Due to the shape anisotropy the magnetization remains along the long axis of nanowire after getting magnetized. These nanowires may be considered as a magnetic dipole. The geometrical arrangement, propinquity of the nanowires and the inter-wire dipolar interactions play a crucial role in the high density data storage applications [**6**]. One useful technique to fabricate such nanowire arrays is electrodeposition, by which metals can be deposited into

the channels of anodic alumina oxide membranes (AAO) [**7-9**]. In an array of magnetic nanowires in a template, the dipolar interactions are negligible for wires with low densities but significantly strong for wires with high densities.

Experimental

Synthesis of cobalt nanowire

Preparation of nanostructures in the ordered pores arrays of alumina membranes under constant potential in various electrolytes have been carried out for over 30 years. Arrays of Co nanowires were fabricated by electrochemical deposition into the nanometer-sized pores. In order to fabricate an array of Co nanowires, one side of the AAO were sputtered with Au by RF sputtering, which acted as the working electrode in a three-electrode electrochemical cell. **Fig. 1** illustrates the three-electrode cell set-up used in this study. A platinum foil and a saturated calomel electrode (SCE) were used as the anode (or counter electrode) and as a potential reference respectively. The electrodeposition solution was restrained to the other side of the membrane so that deposition was initiated onto the Au layer within the pores. The array of Co nanowires was deposited from a solution of 25 gm/L $CoSO_4 \cdot 7H_2O$, 5 gm/L H_3BO_3 and sodium Lauryl Sulphate (SLS), which is used to reduce the surface tension of water for proper wetting of pores. The electrodeposition was carried out at a constant voltage of -1.8 V with respect to counter electrode at room temperature.

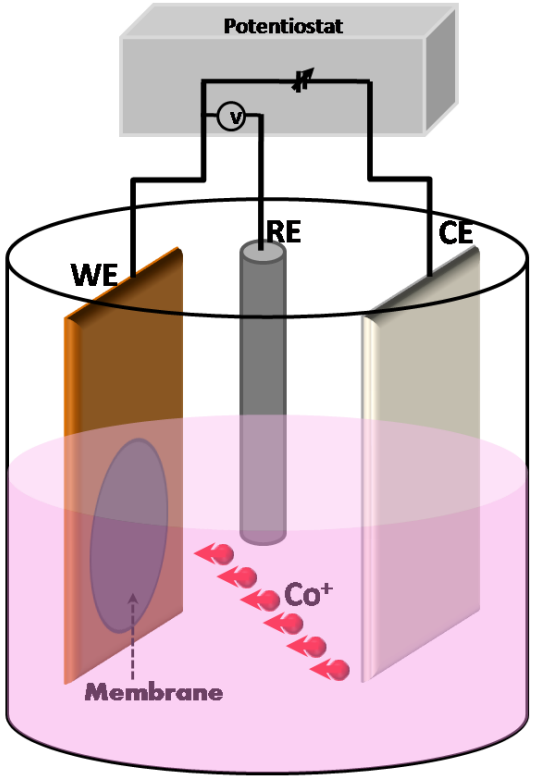

Fig. 1. Schematic representation of three-electrode electrochemical cell setup employed. AAO template mounted electrodes act as a working electrodes (WE), platinum foil counter electrode (CE) and Ag/AgCl/KCl Sat., reference electrode (RE).

To control the crystallography of nanowire, moderate deposition rate is required. For this purpose, voltammetric studies were performed using membranes with 250 nm diameter pores [**10**]. Typical cyclic voltammograms for the CV electro-plating of Co form electrolyte consist 25 gm/L $CoSO_4 \cdot 7H_2O$, 5 gm/L H_3BO_3 and sodium Lauryl Sulphate (SLS) with pH of 4.5 at an AAO template fixed electrode at a scan rate of 100 mVs_{-1} is shown in **Fig. 2**. The anodic and cathodic peaks, a and b, are assigned to oxidation (potential range 0 to 2V) and reduction (0 to -2V) of cobalt inside the nanopores of AAO template, respectively. From the voltammograms, we have chosen the deposition potential -1.8V where the value of reduction current is found ~-0.05A.

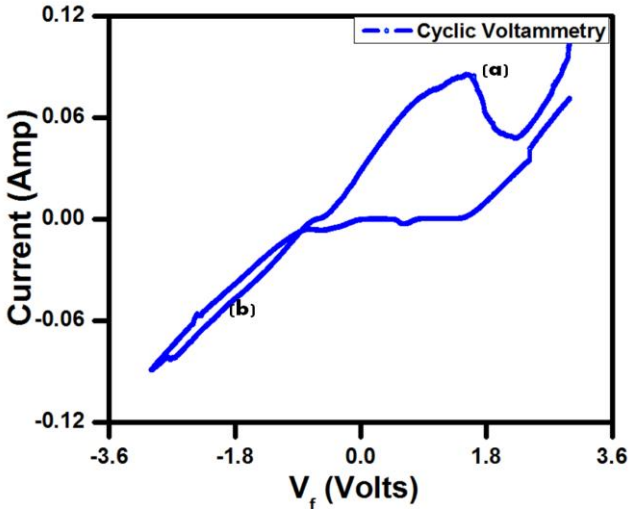

Fig. 2. Cyclic voltammetry curve for the determination of Co nanowire through the pores of AAO template. a and b represent deposition potential the oxidation and reduction of the Co into the nanopores, respectively.

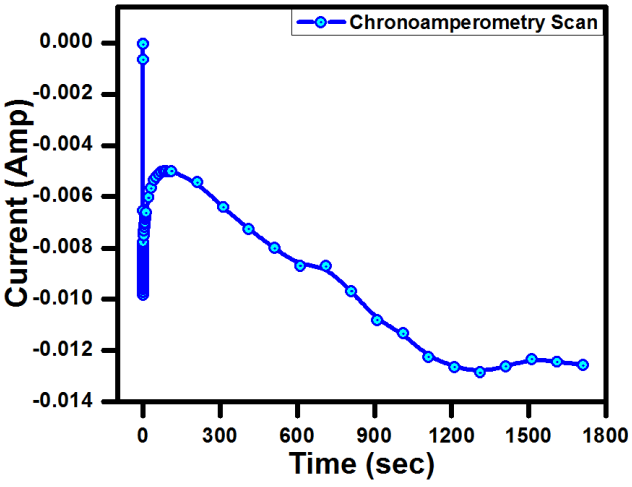

Fig. 3. Chronoamperometric curves recorded during the growth of pristine Co nanowires from the electrolyte with pH value 4.5, at potentials: -1.8V.

Co metal deposited electrochemically into the pores of AAO template by a potentiostatic method for two different times (sample A 1200 sec and sample B 1800 sec) at

applied potentials (−1.8 V/SCE) to get the different length of nanowire. **Fig. 3** shows the chronoamperometric curve between time and current values. It is clearly visualised here that the value of current increases as the time of depositing the Co into the pores increases.

Surface morphology of Co nanowire was investigated by scanning electron microscope (SEM: ZEISS EVO 50) operating at 20 kV accelerating voltage by secondary electron imaging. Cobalt nanowire were scratched from the substrate and ultrasonicated in acetone for 15 min so that Co nanowire could disperse properly. Few drops of the suspension were then transferred on to a carbon coated copper grid and the microstructures were analyzed by high resolution TEM (HRTEM: Technai G20 S-Twin model) operating at 200 kV. X-ray diffraction technique was used to investigate the composition and crystallographic structure of the electrodeposited material (post membranes dissolution). The X-ray diffraction was performed with a monochromatized Cu Kα (λ = 15.4 nm) radiation at 0.5_o glancing angle in $20_o \leqslant 2\theta \leqslant 90_o$ range. The elemental analysis of the samples was carried out by energy dispersive X rays (EDAX) attached to a Scanning transmission electron microscopy (STEM) operating in nanoprobe mode. Magnetic Characterization has been performed by the indigenously made Magneto-optical Kerr Effect (MOKE) and the Electron Paramagnetic resonance.'

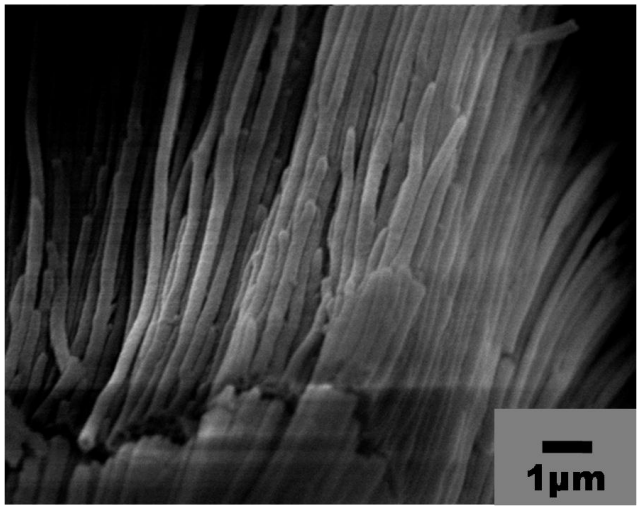

Fig. 4. SEM images electrochemically grown Co nanowires arrays after etching of AAO template. The growth time is 1800 sec.

Results and discussion

Structural and elemental characterization

Scanning electron microscopy (SEM): **Fig. 4** shows typical SEM micrograph of arrays of Co nanowires grown with V = −1.8 V for 1800 sec. It can be clearly seen that the nanowires are vertically aligned and closely packed. The diameters of Co nanowires varies from ~ 250– 300 nm and lengths up to 4-15μm. Earlier the nanowires quite separate due to the AAO template but after etching of the nanowire are very close to each other so the interaction between the nanowire is strong.

Transmission electron microscopy (TEM): **Fig. 5** shows the transmission electron microscopy (TEM) image of electrochemically grown Co nanowires. The diameter measured by TEM is consistent with that obtained from SEM measurements. The length cannot be predicted exactly the same as in SEM, due to the tedious preparation of TEM sample. The nanowire gets broken during the ultrasonication at the time of sample preparation. From the TEM micrograph, it is visualized that there is no residual etched part of AAO template on nanowire. It is also clear from the TEM micrograph that the ultrasoniccation for 15 min is good enough to remove the residual AAO template from the nanowire.

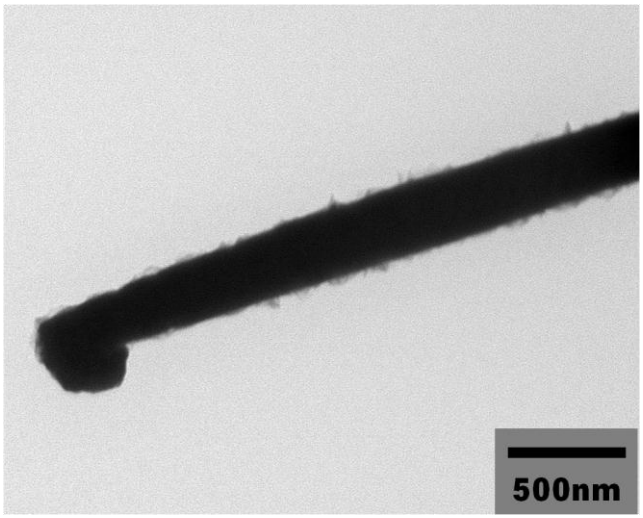

Fig. 5. TEM images electrochemically grown Co nanowires arrays after etching of AAO template.

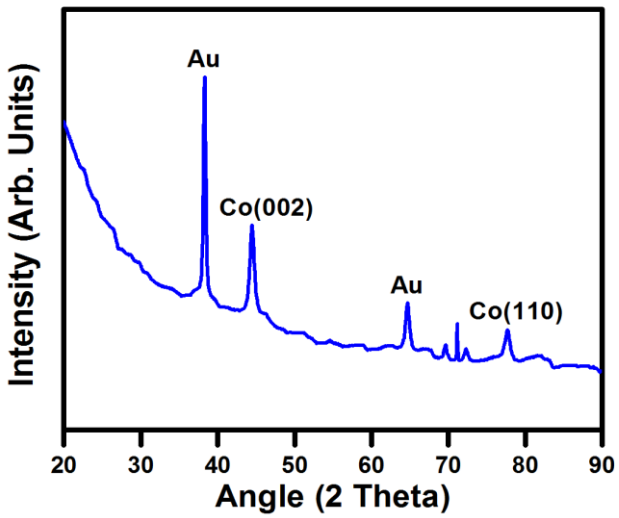

Fig. 6. XRD pattern of nanowire array grown in AAO template.

X-ray diffraction and energy dispersive X-ray spectroscopy (EDX): **Fig. 6** shows the XRD patterns of the electrodeposited Co nanowires sample with AAO template. For the Co nanowire obtained the strong and sharp diffraction peak at $2\theta = 44.4^o$ represents the (002) plane and a weak peak at $2\theta = 77.64^o$ corresponds to (110) reflections

of the hexagonal closely packed (hcp) cobalt lattice respectively from (hcp, PDF-011277). The peak corresponds to (002) with high intensity shows the preferential growth plane while, a weak peak of the (110) plane is observed, which might originate from the not very good crystallization. Further some additional Gold (Au) peaks are also observed. The Au peaks arise from the conducting layer coated on one side of the membrane for electrodeposition. These different peaks observed in plot inferred that Co nanowires are not single crystals but consists of polycrystalline hcp arrangement.

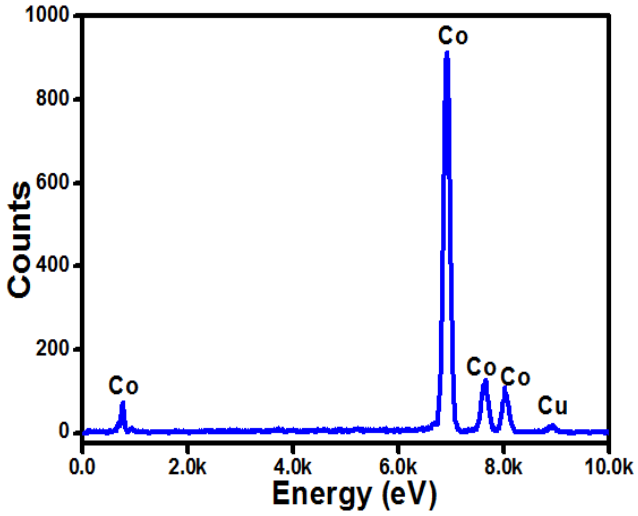

Fig. 7. shows the EDAX spectra of Co nanowire after etching of AAO template.

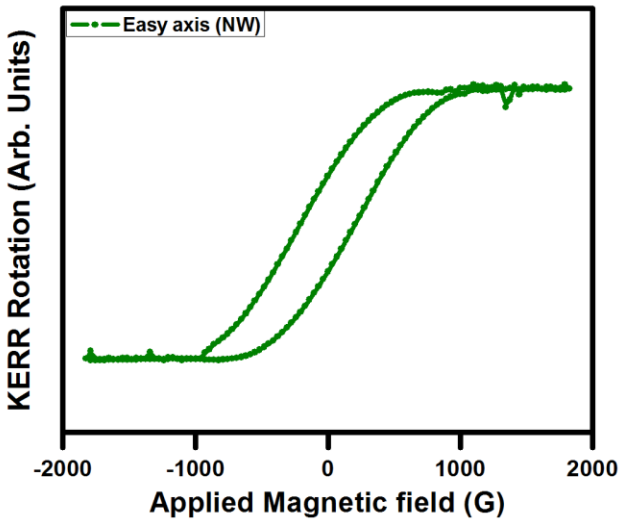

Fig. 8. Hysteresis curve on the Co nanowire arrays with AAO template.

Fig. 7 represents the EDX spectrum for sample containing Co nanowire recorded by the EDX system attached to the TEM. The spectrum clearly shows the presence of Cobalt in the sample along with copper. In this sample, copper has come from the sample support grid TEM studies.

Magnetic characterization

Magneto-optical Kerr effect: Hysteresis loops are measured by the magneto-optical Kerr effect (MOKE) at normal incident [**11-13**]. Since Co nanowires were partially embedded in Alumina which was transparent at optical frequencies (He–Ne laser at 632.8 nm), the MOKE signal was relatively weak due to the roughness of Co nanowire along with AAO template. **Fig. 8** shows the easy axis of Co nanowire arrays within the AAO template measured by MOKE. The coercivity and Hk is found ~ 200 G and ~1022 G respectively. The MOKE measurement on the electrodeposited nanowire is very tedious because of the sample preparation. We have used the chemical mechanical polishing (CMP) for smoothing of the nanowire sample. The AFM image confirms that the MOKE signal is directly coming from the nanowire surface as shown in the **Fig. 9**. The AFM profile confirms the diameter of the nanowire.

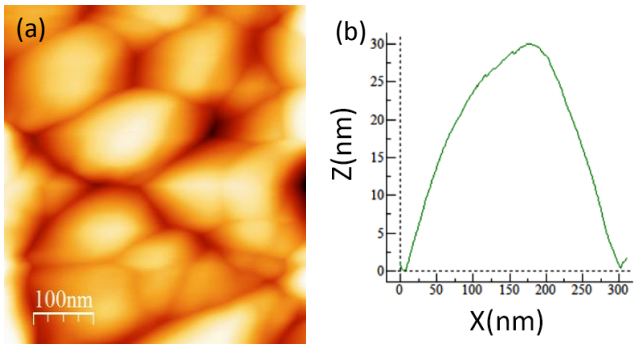

Fig. 9. (a) AFM image and profile on the polished surface of Co nanowire arrays with (b) AAO template.

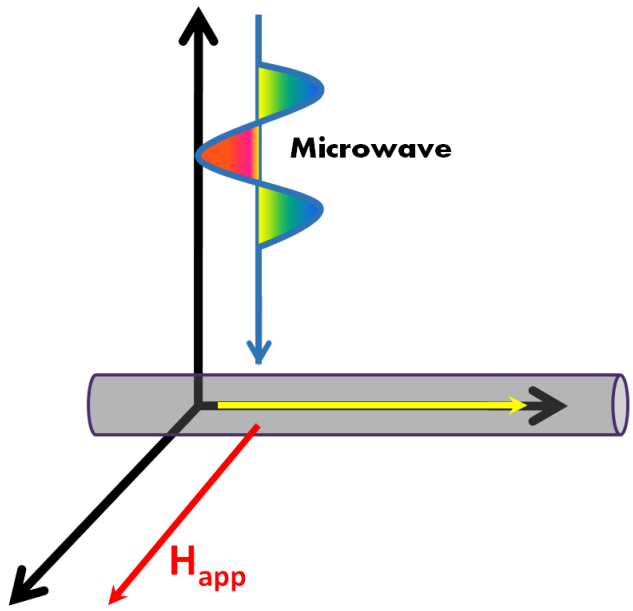

Fig. 10. Schematic representation of EPR on co nanowire.

Electron spin resonance

The ferromagnetic resonance spectrum measured by electron paramagnetic resonance (EPR) at room temperature with microwave of frequency 9.8GHz and bias

field applied parallel and perpendicular to the Co nanowires axis [**14**]. The measured feeromagnetic resonance signal was proportional to the first derivative of the imaginary part of the magnetic susceptibility. The microwave power in the cavity was equal to 0.96 mW, and the modulation frequency was 100 kHz. The microwave signal was weak, because of the small amount of magnetic material was present for the measurements. FMR measurements of these structures indicate that the resonance fields are weakly affected by the aspect ratio and but strongly depends on the interaction between these nanostructures and the temperature. **Fig. 10** shows the schematic diagram for electron paramagnetic resonance on the single nanowire. The easy axis of nanowire, microwave and applied magnetic field are mutually perpendicular in our case.

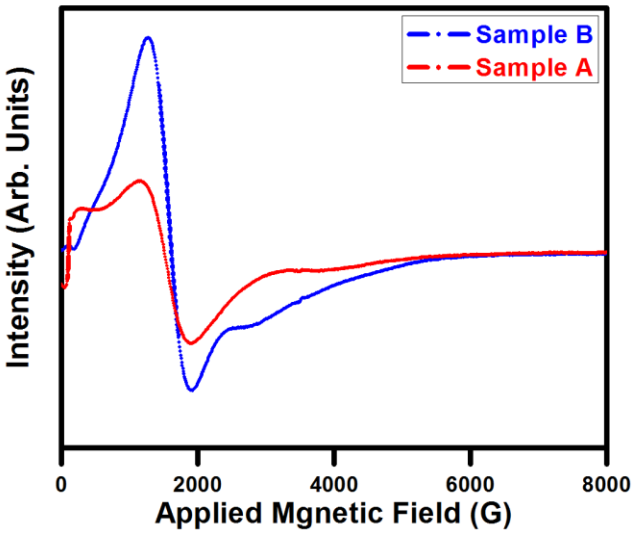

Fig. 11. ESR/FMR spectra of single element Co nanowire arrays for two different length at room temperature.

From the EPR spectrum the difference in intensity of sample A and sample B is may be due to the different length of Co nanowires in the AAO. Intensity is proportional to the amount of the ferromagnetic material in the samples. The ratio of the intensity was ~1:2, which is in agreement with our deposition condition. The resonance has been observed in the sample A with 5µm length at 1510 G and for sample B with 11µm at 1618 G. The field is shifted slowly with length but it strongly depends on the interaction between the nanowires as we have found in micro-magnetic simulations. One more peak is observed in this spectrum at 3510 G for both the samples and, it is not variable with the length. It is the characteristic feature of Co material for EPR measurement (**Fig. 11**).

Simulation

The object oriented micro-magnetic framework OOMMF obtained from The National Institute of Standards and Technology is a fantabulous tool for simulation of micro-magnetic problems [**15-18**]. The evolution of the magnetization distribution is obtained by solving the Landau–Lifshitz Gilbert (LLG) ordinary differential equation:

$$\frac{dM}{dt} = -\gamma M \times H_{eff} - \alpha \frac{\gamma}{M_s} M \times (M \times H_{eff})$$

The field-dependent behaviour of a single cobalt nanowire with dimensions of 300 nm × 300 nm × L nm (different length) is simulated with a cell size of 10 nm × 10 nm × 20 nm. The cuboid mesh has been choosen to perform the more realistic situation to the micromagnetic simulation. The standard cobalt parameters are: saturation magnetization Ms = 1.4 × 10_6 A m−1, exchange coupling constant A = 1.4 ×10_{-12} J m−1 and uniaxial anisotropy K_1 has been taken zero because of the polycrystalline nature of the nanowire. The damping parameter α is set to 0.5.

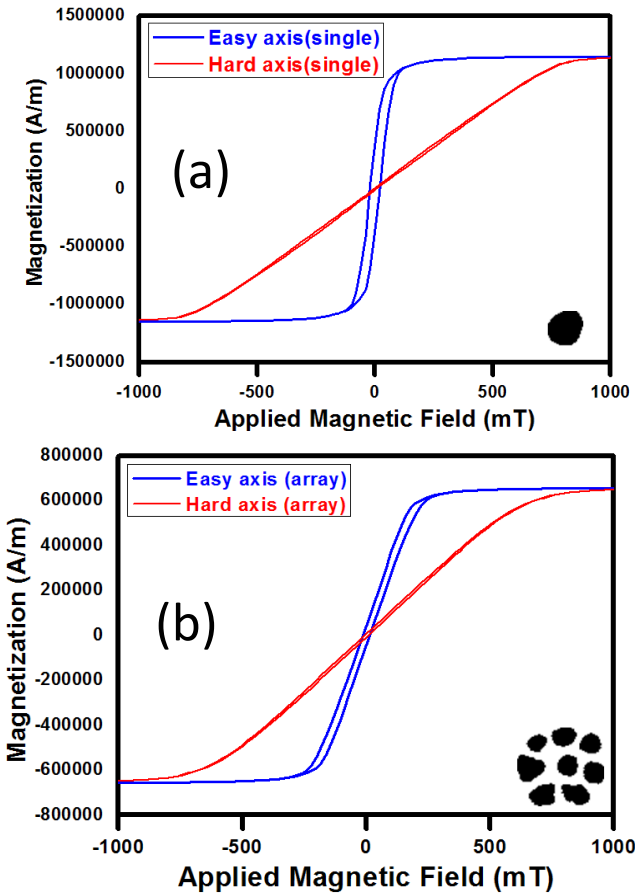

Fig. 12. Easy and Hard axis Hysteresis curve of (a) single and (b) array of eight Co nanowire using micromagnetic simulation package (OOMMF).

We have performed the micromagnetic simulation for different length (L = 1.5, 3.0, 5.0, 10.0, 15.0, 20.0 and 25.0µm). **Fig. 12** shows the simulated hysteresis curve for single and arrays of eight Co nanowire with the L = 1500 nm. The images in inset shows the bmp files generated from the SEM images of the top of the nanowire which is used for simulations. From the curve it is clearly observed that the effect of interaction between the nanowires plays an important role on shape of hysteresis curve. The difference between simulated and experimental results is

due to the number of nanowires. For single nanowire coercivity variation with nanowire length has been shown in **Fig. 13**.

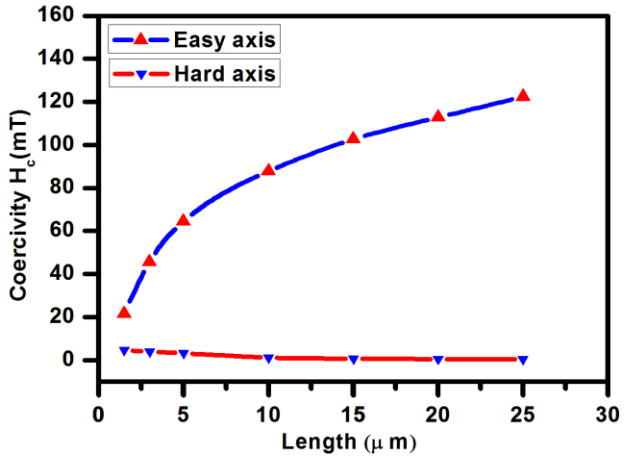

Fig. 13. Easy and Hard axis variation of Coercivity with length of single Co nanowire using micromagnetic simulation package (OOMMF).

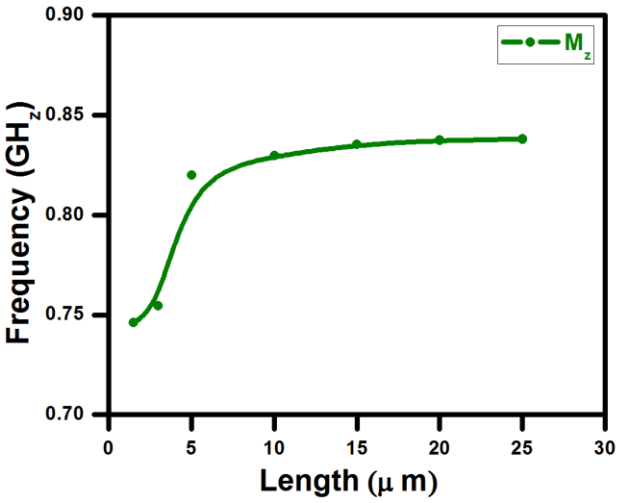

Fig. 14. Variation of resonance frequency with length of single Co nanowire using micromagnetic simulation package (OOMMF).

We have also performed the micro-magnetic simulation to understand the dynamic behaviour of the nanowire with respect to the length of the nanowire. **Fig. 14** shows the variation of resonance frequency in single Co nanowire. The very small variation in the resonance frequency is found in the range of 1-10μm for the 0.2T magnetic field in the transverse direction.

We have performed the dynamic simulation for the array of eight nanowires. It is speculated that the resonance frequency has been affected by the interaction of the surrounding nanowires. The resonance frequency is increased from 0.7 GHz to 1.1 GHz due to the interaction effect for 0.2 T magnetic fields.

Conclusion

The Co nanowire arrays to make perpendicular magnetic recording media were fabricated with nanoporous anodic aluminum oxide (AAO) templates by electrodeposition. The results show that the diameters of Co nanowires in AAO templates are about to 300 nm and with variable lengths about 4-15μm are adjusted by changing the time of deposition. The magnetic properties of the prepared nanowires are different under different electrodepositing conditions. The effect of aspect ratio on the static and dynamic properties of Co nanowire arrays was determined by the MOKE method and FMR measurement. The MOKE technique was based on direct measurement from the Co nanowire. The length dependence of coercivity and the resonance frequency in FMR for Co nanowire has been shown by using micromagnetic modelling.

Acknowledgments

The authors gratefully acknowledge use of the AFM Facility and also the Central SEM Facility of IIT Delhi. The authors thank Dr. R. P. Pant for Electron Paramagnetic Resonance measurements in National Physical Laboratory Delhi. Also one of the authors would like to acknowledge CSIR-UGC for providing him scholarship.

Reference

1. Ge, S.; Li, C.; Ma, X.; Li, W.; Xi, L.; Li, C. X. J. Appl. Phys. **2001**, 90, 509. **DOI:** 10.1063/1.1327599.
2. Hamrakulov, B.; Kim, I.-S.; Lee, M. G.; Park, B. H. Trans. Nonferrs Met. Soci. Chi. **2009**, 19, 83. **DOI:** 10.1016/S1003-6326(10)60250-6.
3. Yong, R.; Jianbo, W.; Qingfang, L.; Bin, Z.; Xianghua, H.; Desheng, X. J. Phys. D: App. Phys. **2009**, 42, 105002. **DOI:** 10.1088/0022-3727/42/10/105002.
4. Reich, D. H.; Tanase, M.; Hultgren, A.; Bauer, L. A.; Chen, C. S.; Meyer, G. J. J. Appl. Phys. **2003**, 93, 7275. **DOI:** 10.1063/1.1558672.
5. Wanekaya, A. K.; Chen, W.; Myung, N. V.; Mulchandani, A. Electroanalysis **2006**, 18, 533. **DOI:** 10.1002/elan.200503449.
6. Kou, X.; Fan, X.; Dumas, R. K.; Lu, Q.; Zhang, Y.; Zhu, H.; Zhang, X.; Liu, K.; Xiao, J. Q. Adv. Mat. **2011**, 23, 1393. **DOI:** 10.1002/adma.201003749.
7. Kartopu, G.; Yalçın, O.; Kazan, S.; Aktaş, B. JMMM **2009**, 321, 1142. **DOI:** 10.1016/j.jmmm.2008.10.039.
8. Pirota, K. R.; Navas, D.; Hernández-Vélez, M.; Nielsch, K.; Vázquez, M. J. All. Comp. **2004**, 369, 18. **DOI:** 10.1016/j.jallcom.2003.09.040.
9. Kim, K. T.; Cho, S. M. Mat. Lett. **2006**, 60, 352. **DOI:** 10.1016/j.matlet.2005.08.064.
10. Sun, X.-Y.; Xu, F.-Q.; Li, Z.-M.; Zhang, W.-H. Mat. Chem. Phys. **2005**, 90, 69. **DOI:** 10.1016/j.matchemphys.2004.10.007.
11. Keatley, P. S.; Kruglyak, V. V.; Hicken, R. J.; Childress, J. R.; Katine, J. A. JMMM **2006**, 306, 298. **DOI:** 10.1016/j.jmmm.2006.03.030.
12. Savoini, M.; Ciccacci, F.; Duo, L.; Finazzi, M. Rev. Sci. Instr. **2011**, 82, 023709. **DOI:** 10.1063/1.3555757.
13. Wuxia, L.; Yong, P.; Jun, Z.; Grenville, A. J.; Tiehan, H. S. J. Phys: Con. Seri. **2005**, 17, 20. **DOI:** 10.1088/1742-6596/17/1/004.
14. Vázquez, M.; Hernández-Vélez, M.; Pirota, K.; Asenjo, A.; Navas, D.; Velázquez, J.; Vargas, P.; Ramos, C. EPJB **2004**, 40, 489. **DOI:** 10.1140/epjb/e2004-00163-4.
15. Liu, R.; Wang, J.; Liu, Q.; Wang, H.; Jiang, C. J. Appl. Phys. **2008**, 103, 013910. **DOI:** 10.1063/1.2829817.
16. Subramani, A.; Geerpuram, D.; Domanowski, A.; Baskaran, V.; Metlushko, V. Physica C: Superconductivity **2004**, 404, 241. **DOI:** 10.1016/j.physc.2003.11.044.
17. Verma, L. K.; Ng, V. JMMM **2007**, 313, 317. **DOI:** 10.1016/j.jmmm.2007.01.019.
18. Rahman, I. Z.; Boboc, A.; Razeeb, K. M.; Rahman, M. A. JMMM

2005, 290-291, Part 1, 246.
DOI: 10.1016/j.jmmm.2004.11.193.